Journal of Porphyrins and Phthalocyanines
J. Porphyrins Phthalocyanines 2011; **15**: 973–983
DOI: 10.1142/S1088424611003902

Published at http://www.worldscinet.com/jpp/

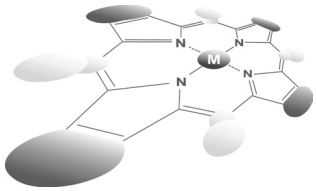

Synthesis and toxicity of cobaltabisdicarbollide-containing porphyrins of high boron content

N.V.S. Dinesh K. Bhupathiraju[a], Vijay Gottumukkala[a], Erhong Hao[b], Xiaoke Hu[a◊◊], Frank R. Fronczek[a], David G. Baker[c], Nobuko Wakamatsu[c] and M. Graça H. Vicente*[a◊]

[a] *Department of Chemistry, Louisiana State University, Baton Rouge, LA 70803, USA*
[b] *Anhui Key Laboratory of Functional Molecular Solids and Anhui Key Laboratory of Molecular Based Materials, College of Chemistry and Material Science, Anhui Normal University, Wuhu, Anhui 241000, China*
[c] *Department of Pathobiological Sciences, School of Veterinary Medicine, Louisiana State University, Baton Rouge, LA 70803, USA*

Dedicated to Professor Karl M. Kadish on the occasion of his 65th birthday

Received 17 May 2011
Accepted 24 June 2011

ABSTRACT: Two porphyrins of high boron content (OCP and HCP–PEG) were prepared in high yields from the reaction of the corresponding tri- and tetra-(dihydroxyphenyl)porphyrins with zwitterionic cobaltabisdicarbollide [3,3′-Co(8-$C_4H_8O_2$-1,2-$C_2B_9H_{10}$)(1′,2′-$C_2B_9H_{11}$)]. Both porphyrins were found to have low cytotoxicity toward human HEp2 cells, and to localize subcellularly mainly in the cell lysosomes. Animal toxicity investigations using male and female BALB/c mice also revealed low toxicity for both compounds. The determined maximum tolerated dose (MTD) for these boronated porphyrins administered intraperitoneally were 160 mg/kg for OCP and 320 mg/kg for HCP–PEG. Our studies warrant further development of these porphyrins of high boron content, and in particular of HCP–PEG, as boron delivery vehicles for BNCT.

KEYWORDS: cobaltabisdicarbollide, porphyrin, BNCT, PDT, toxicity.

INTRODUCTION

Boronated porphyrins of high boron content and low toxicity can find application as boron delivery agents for boron neutron capture therapy (BNCT) of tumors [1]. BNCT is a binary therapy that involves the irradiation of ^{10}B-rich tumors with low energy neutrons; this produces high linear energy transfer (high-LET) alpha-particles and recoiling lithium-7 nuclei, and releases 2.4 MeV of kinetic energy, according to the equation:

$$^{10}B + {}^{1}n \rightarrow {}^{7}Li^{3+} + {}^{4}He^{2+} + \gamma + 2.4\ MeV \qquad (1)$$

The high-LET particles are highly cytotoxic and due to their limited path lengths in tissue (less than 10 μm) BNCT has the potential to be a highly selective and localized cancer therapy, destroying ^{10}B-containing tumor cells in the presence of normal boron-free cells. Therefore, research in the last two decades has centered on the discovery of tumor-selective boronated agents able to deliver therapeutic boron concentrations (15–30 μg/g tumor) to targeted tumors with minimal normal tissue toxicity [2]. Two compounds are currently in BNCT clinical trials for brain tumors, melanomas, and squamous cell carcinomas: sodium mercaptoundecahydro-*closo*-dodecaborate (BSH) and (*L*)-4-dihydroxy-borylphenylalanine (BPA), shown in Fig. 1 [3]. While BSH and BPA have shown some effectiveness and low toxicity as boron delivery agents for BNCT, both of these compounds have only moderate selectivity and low retention times in tumors. On the other hand, boronated porphyrin derivatives, in particular those of high boron content, could potentially deliver higher amounts of boron to tumors at the same boron dose, with increased selectivity and retention time

◊SPP full and ◊◊student member in good standing

*Correspondence to: M. Graça H. Vicente, email: vicente@lsu.edu, tel: +1 225-578-7442

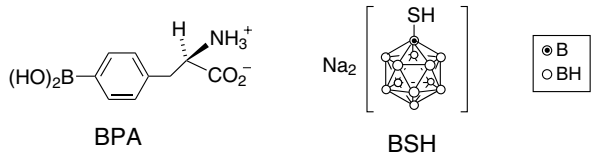

Fig. 1. Structures of BSH and BPA currently in BNCT clinical trials

in tumor tissue [4]. Furthermore, boronated porphyrins retain the absorption and emission properties characteristic of this type of molecule, facilitating the quantification of tumor-localized boron and treatment planning. However, the synthesis of boronated porphyrins of high boron content often leads to low yields of the target products, due to steric and/or electronic reasons. We have recently developed an efficient methodology for the preparation of cobaltabisdicarbollide-containing porphyrins, based on the opening of the dioxane ring of zwiterionic [3,3′-Co(8-$C_4H_8O_2$-1,2-$C_2B_9H_{10}$)(1′,2′-$C_2B_9H_{11}$)] by pyridyl- or phenoxy-containing porhyrin macrocycles [5]. Using this strategy, we have prepared OCP (**1**), containing 39% boron by weight, in one step from commercially available tetra(3,5-dihydroxyphenyl)porphyrin, in 95% yield (Scheme 1) [5c]. Preliminary cellular investigations showed that OCP had low cytotoxicity toward human HEp2 cells [5c] and that a pegylated cobaltabisdicarbollide-porphyrin of comparatively low boron content (24%) conjugated to a cell penetrating peptide (from the human immunodeficiency virus I transcriptional activator, HIV-1 Tat 48–60), readily accumulated within cells, about 11-fold compared to the non-conjugated porphyrin [5d]. Herein we describe the synthesis of an unsymmetric high boron-containing porphyrin designated HCP–PEG (**2**) which is 34% boron by weight, bearing twelve (rather than six) boron cages and one PEG chain, and evaluate its cytotoxicity and cellular uptake in human HEp2 cells. We also investigated and compared the toxicity of OCP and HCP–PEG in BALB/c mice. The low toxicity found for these boronated porphyrins of high boron content, and in particular for HCP–PEG, is crucial in their further development and investigation as boron delivery vehicles for BNCT.

RESULTS AND DISCUSSION

Synthesis

While symmetrically substituted OCP (**1**) is readily prepared in a one-step reaction from commercially available tetra(3,5-dihydroxyphenyl)porphyrin, as shown in Scheme 1, the unsymmetric HCP–PEG (**2**) required initial synthesis of a porphyrin containing two different phenyl substituents, *i.e.*, porphyrins **3a–c**, as shown in Scheme 2. A mixed-aldehyde condensation using 3 equiv. of 3,5-dimethoxybenzaldehyde, 1.5 equiv. of an appropriately *para*-functionalized benzaldehyde and 4 equiv. of pyrrole under Lindsey's reaction conditions [6], produced the corresponding A_3B-type porphyrin as the major product, in yields ranging from 9–12%. Crystals of porphyrins **3a–c** suitable for X-ray analysis were grown from slow evaporation of dichloromethane and hexane. The molecular structures for these three porphyrins are shown in Fig. 2. In all porphyrins, the 24-atom porphyrin core is fairly planar. In both **3a** and **3c**, there is a slight saddle distortion, with maximum and mean deviations 0.254(2) and 0.091 Å for **3a**; 0.279(2) and 0.104 Å for **3c**.

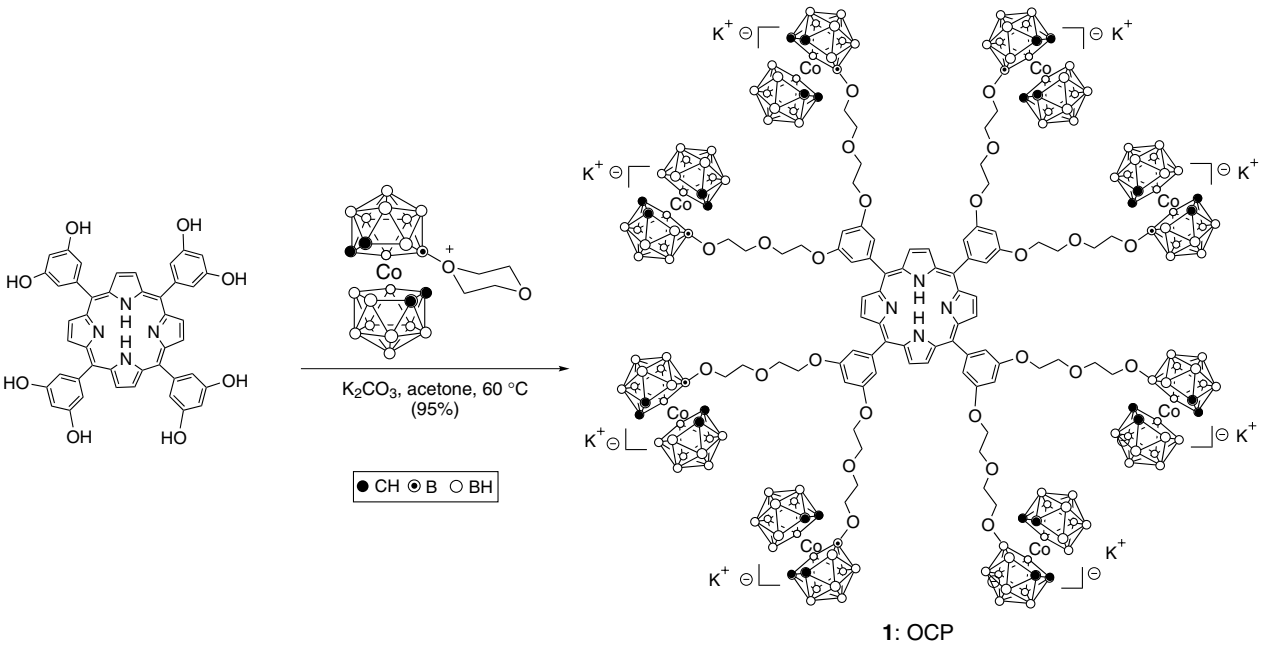

Scheme 1. One-step synthesis of octa-cobaltacarboranylporphyrin (OCP)

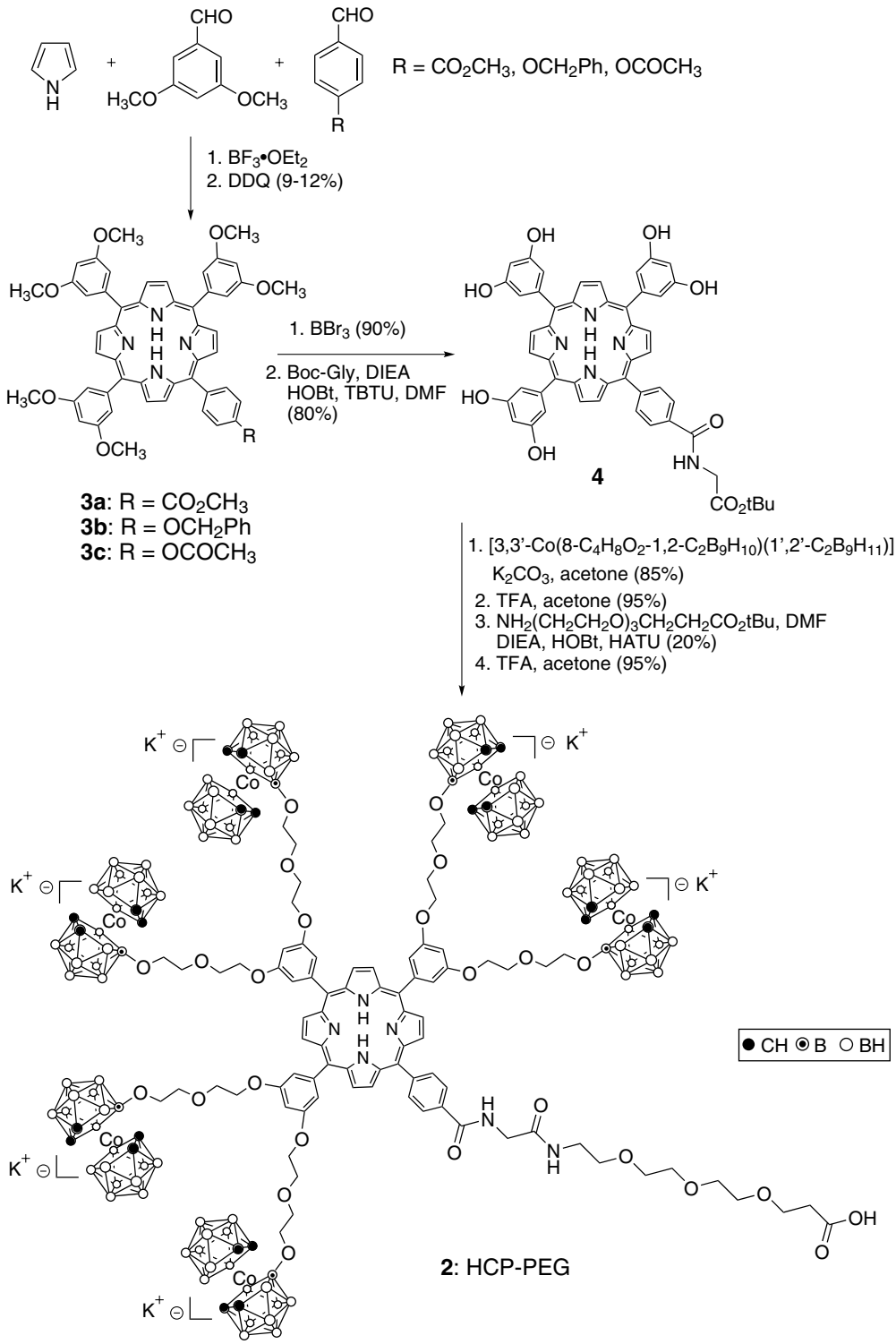

Scheme 2. Synthesis of hexa-cobaltacarboranylporphyrin-PEG (HCP–PEG)

For **3b**, the distortion from planarity is smaller, with maximum and mean deviations 0.111(3) and 0.036 Å. The conformations of the methoxy groups in **3a** and **3c** are also similar, five pointing away from the center of the molecule and one inward in both, while in **3b**, five point inward and only one outward.

Deprotection of the methoxyl groups of porphyrins **3a–c** using BBr_3 [5d] also cleaved the methyl ester group of porphyrin **3a**, and the benzyl and acetyl ethers of porphyrins **3b** and **3c**, respectively. The free carboxylic acid group resulting from deprotection of porphyrin **3a** reacted with Boc-protected glycine in the presence of HOBt and TBTU as coupling agents [7] to afford porphyrin **4** in 80% yield. The glycine linker decreases steric interactions and increases the yield of the conjugation reaction to the PEG group [8]. Reaction of porphyrin **4** with

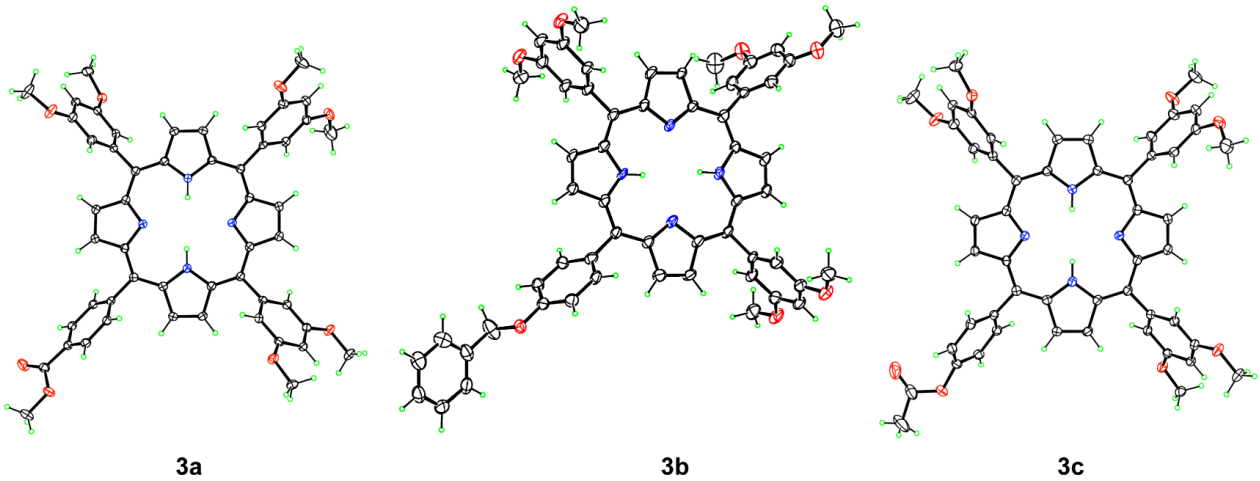

Fig. 2. Molecular structures of porphyrins **3a**, **3b**, and **3c** with 50% ellipsoids

zwiterionic cobaltabisdicarbollide [3,3′-Co(8-$C_4H_8O_2$-1,2-$C_2B_9H_{10}$)(1′,2′-$C_2B_9H_{11}$)], prepared from reaction of commercially available Cs[Co($C_2B_9H_{11}$)$_2$] with 1,4-dioxane in the presence of BF_3·Et_2O [9], gave the corresponding hexacobaltacarboranylporphyrin in 85% yield. Deprotection of the *tert*-butyl ester group using TFA proceeded nearly quantitatively, and the resulting carboxylated porphyrin was characterized by NMR, MS and UV-vis. Subsequent conjugation of this porphyrin to commercially available *tert*-butyl-12-amino-4,7,10-trioxadodecanoate followed by deprotection of the *tert*-butyl group using TFA, gave HCP–PEG (**2**) in 15% overall yield from porphyrin **4**. HCP–PEG is a valuable precursor for the conjugation of various biomolecules, such as the HIV-1 Tat 48–60 peptide [5d], that might enhance tumor cell uptake and overall biological efficacy of the boronated porphyrin as BNCT delivery agent [2b].

Cell studies

The subcellular distribution and cytotoxicity of OCP (**1**) and HCP–PEG (**2**) were evaluated in human carcinoma HEp2 cells and the results obtained using HCP–PEG are shown in Figs 3 and 4 (we have previously published the results for OCP [5c]). At concentrations up to 50 μM for OCP (higher concentrations were not evaluated to avoid precipitation due to compound aggregation [5c]) and up to 400 μM for HCP–PEG in the dark, the compounds were found non-toxic to the cells, as evaluated using the Cell Titer Blue assay [10] (Fig. 3a). Upon exposure to approx. 1 J/cm^2 light dose, neither compound was found to be toxic, as shown in Fig. 3b for HCP–PEG. Fluorescence microscopy was used to investigate cellular uptake and subcellular localization, as previously reported for OCP [5c] and shown in Fig. 4 for HCP–PEG. As observed for OCP [5c], HCP–PEG showed a punctuate pattern that correlated mostly with the cell lysosomes, as seen in Fig. 4j. A minor/partial site of localization was the Golgi apparatus. Preferential lysosomal localization of cobaltabisdicarbollide-containing porphyrins [5b–d] and other boronated porphyrins [11, 12] might result from endocytosis of small porphyrin aggregates and their subsequent localization in endosomal vesicles, some of which might fuse with the cell lysosomes.

Animal toxicity

Both male and female BALB/c mice were used in these studies, as previously reported for other boronated

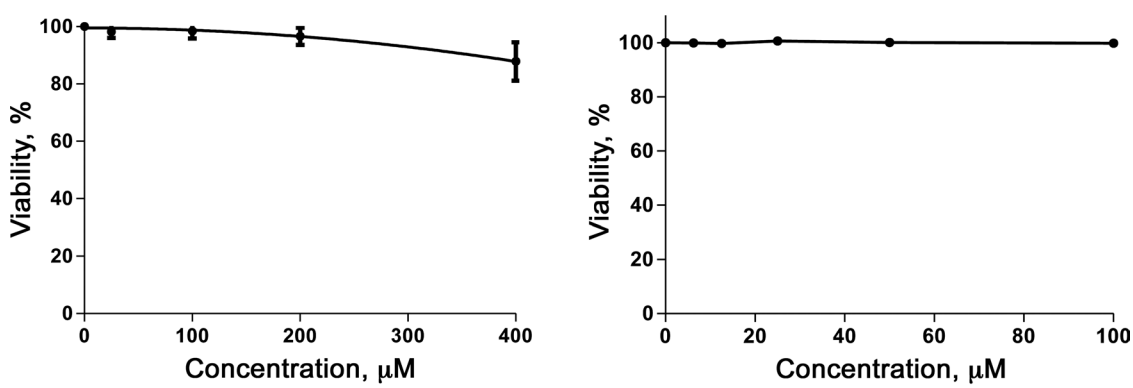

Fig. 3. Cytotoxicity of HCP–PEG (**2**) toward HEp2 cells using the Cell Titer Blue assay, (a) in the dark and (b) after exposure to 1 J/cm^2 light dose

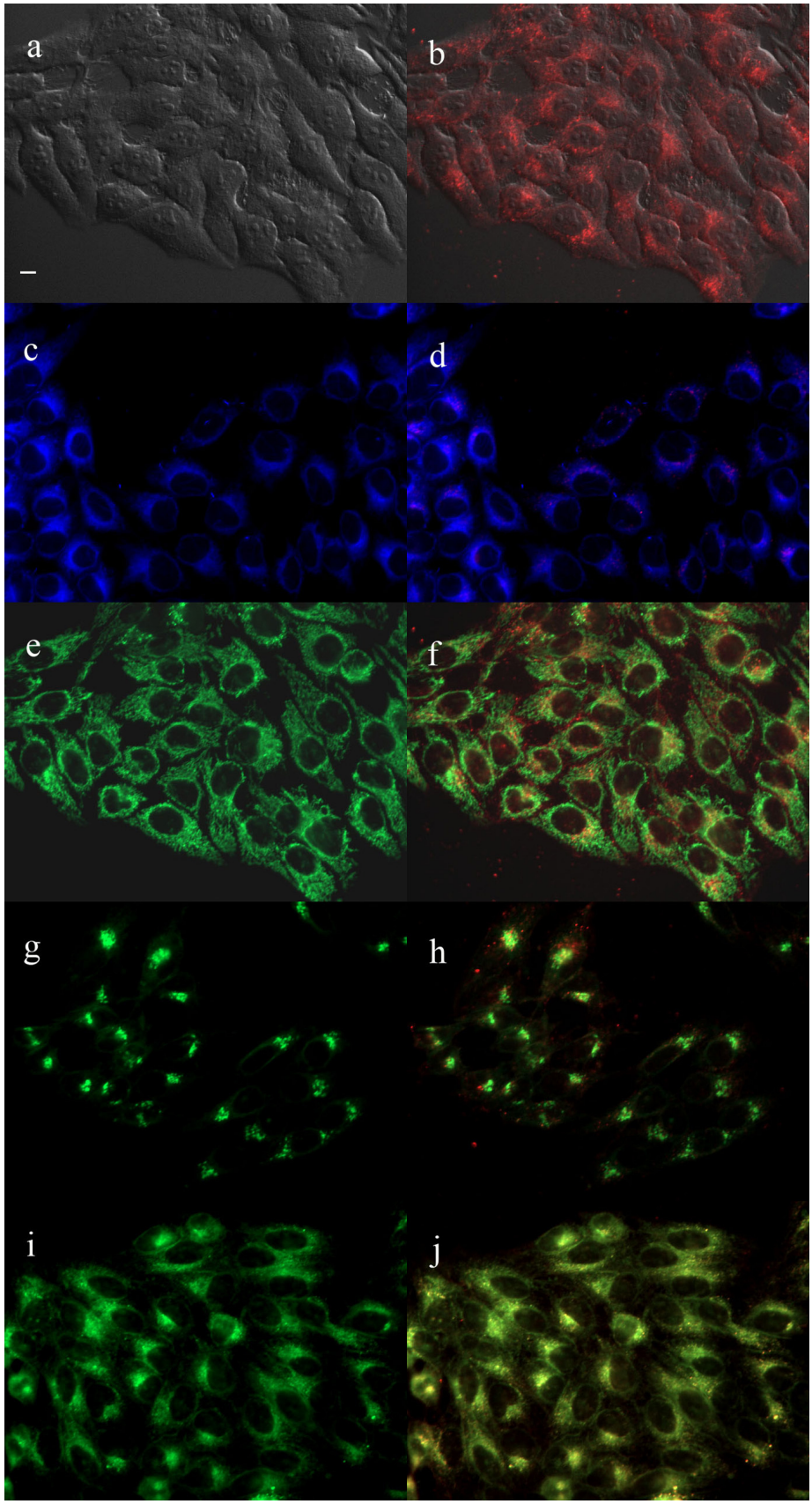

Fig. 4. Subcellular localization of HCP–PEG (**2**) in HEp2 cells at 10 μM for 6 h; (a) phase contrast, (b) overlay of HCP–PEG fluorescence and phase contrast, (c) ER tracker Blue/White fluorescence, (e) MitoTracker Green fluorescence, (g) BODIPY Ceramide, (i) LysoSensor Green fluorescence, and (d, f, h, j) overlays of organelle tracers with HCP–PEG fluorescence. Scale bar: 10 μm

porphyrins [11c]. OCP or HCP–PEG were dissolved in 3% DMSO in PBS and all mice received intraperitoneal (ip) injections of 0.15–0.74 mL. Group 6 received a maximum dose of 160 mg/kg of compound OCP (**1**), representing maximum saturation of 4 mg/mL. Group 12 received maximum dose of 320 mg/kg of HCP–PEG (**2**), representing maximum saturation of 20 mg/mL. No clinical chemistry changes occurred corresponding to either vehicle or compound injected. Tables 1 and 2 show the clinical data obtained for OCP and HCP–PEG, respectively.

No signs of toxicity were observed in any of the experiments using HCP–PEG or OCP. For OCP the slightly elevated glucose levels in Table 1 might indicate a diabetic condition, or may simply occur due to excitement and increased corticosteroid release. The latter is considered responsible for increases in serum glucose levels observed in mice of group 3. On the other hand, the trends toward decreases in total protein, albumin, and globulin may be explained by decreased production or increased loss. With HCP–PEG (Table 2) plasma glucose levels generally increased, likely due to excitement and increase corticosteroid release. One mouse in group 7 (control) and both mice in group 9 (40 mg/kg) had highly elevated plasma AST levels, most likely due to liver trauma during compound injection. Values for both mice in group 12 (320 mg/kg) were moderately elevated possibly suggestive of mild hepatocyte damage though this was not observed histologically. A more likely explanation for the moderate elevations in mice of group 12 was muscular overexertion. One mouse in each of groups 8 and 9 (20 and 40 mg/kg, respectively) had mildly elevated plasma ALT levels. One of these mice (from group 9) also showed elevated AST levels. These mild elevations were likely due to trauma to the liver during compound injection. Overall, there did not appear to be a treatment effect on ALT. Plasma alkaline phosphatase levels were within normal limits suggestive of a lack of toxicity for several of the major organ systems including the renal, gastrohepatic, immune, and skeletal systems. Plasma bilirubin levels were within normal limits. Plasma total protein levels plateaued in mice of group 11 (160 mg/kg) and declined slightly in mice of group 12 (320 mg/kg) most likely because of reductions in albumin levels. However, levels of total protein in all mice remained within normal limits. Plasma albumin levels declined slightly in mice of group 12 (320 mg/kg) but remained within normal limits. No treatment effects were noted in plasma globulin levels. The values for all mice were within normal limits. Histopathologic examination revealed no lesions attributable to compound administration. Extramedullary hematopoiesis was observed in all mice, and may represent mild levels of stress, normal for these animals. Moderate thickening of Bowman's capsule (periglomerular fibrosis) was also observed in one renal glomerulus of one mouse in group 2 and likely represented an incidental finding.

Table 1. Serum chemistry values for 11 BALB/c mice administered OCP (**1**) in 3% DMSO in PBS (groups 2, 3, 4, 5, 6) or only 3% DMSO in PBS (vehicle: group 1), by ip injection

Group	**1**	**2**	**3**	**4**	**5**	**6**
Glucose	190.0	212.0[a]	258.0[b]	217.5[a]	211.0[a]	219.0[a]
(mg/dl)	(0)	(8.0)	(5.0)	(0.5)	(6.0)	(7.0)
AST	92.0	577.0	150.5	282.5	244.5	224.5
(U/L)	(0)	(468.0)	(87.5)	(178.5)	(156.5)	(61.5)
ALT	26.0	319.0	68.5	289.0	199.0	185.5
(U/L)	(0)	(260.0)	(21.5)	(257.0)	(130.0)	(20.5)
AP	114.0	117.5	158.5	127.0	170.5	138.5
(U/L)	(0)	(11.5)	(31.5)	(3.0)	(11.5)	(8.5)
Bilirubin	0.10	0.15	0.15	0.15	0.1	0.2
(mg/dl)	(0)	(0.05)	(0.05)	(0.05)	(0)	(0)
Total Prot.	5.0	4.6	4.7	4.75	4.6	4.4
(g/dl)	(0)	(0)	(0.1)	(0.05)	(0.1)	(0.2)
Albumin	2.9	2.6	2.75	2.7	2.7	2.55
(g/dl)	(0)	(0.1)	(0.05)	(0.1)	(0)	(0.05)
Globulin	2.1	2.0	1.95	2.05	1.9	1.85
(g/dl)	(0)	(0.1)	(0.05)	(0.05)	(0.1)	(0.15)
BUN	20.0	18.5	19.5	15.5	22.5	18.0
(mg/dl)	(0)	(1.5)	(0.5)	(0.5)	(3.5)	(4.0)

Values represent mean serum chemistry levels and the standard error of the mean (SEM) values are given in parenthesis. For individual analytes measured, rows with superscripts in common (a or b) are not different from one another ($p > 0.05$).

Table 2. Serum chemistry values for 12 BALB/c mice administered HCP–PEG (**2**) in 3% DMSO in PBS (groups 8, 9, 10, 11, 12) or only 3% DMSO in PBS (vehicle: group 7), by ip injection

Group	**7**	**8**	**9**	**10**	**11**	**12**
Glucose	150.0	166.0	227.5	140.5	137.0	151.5
(mg/dl)	(6.0)	(19.0)	(37.5)	(0.5)	(6.0)	(3.5)
AST	1049.0	207.7	2248.5	147.5	146.5	589.5
(U/L)	(947.0)	(201.35)	(1006.5)	(80.5)	(8.5)	(294.5)
ALT	159.5	244.0	337.0	28.5	26.5	125.5
(U/L)	(135.5)	(175.0)	(142.0)	(6.5)	(1.5)	(74.5)
AP	116.5	112.0	130.0	125.5	108.0	152.0
(U/L)	(17.5)	(7.0)	(10.0)	(17.5)	(12.0)	(49.0)
Bilirubin	0.30	0.20	0.40	0.20	0.20	0.30
(mg/dl)	(0.05)	(0.0)	(0.0)	(0.05)	(0.0)	(0.05)
Total Prot.	5.4	5.0	5.5	5.9	5.9	5.4
(g/dl)	(0.45)	(0.05)	(0.05)	(0.15)	(0.45)	(0.20)
Albumin	3.1	2.8	3.2	3.3	3.4	3.0
(g/dl)	(0.30)	(0.0)	(0.0)	(0.05)	(0.15)	(0.15)
Globulin	2.3	2.2	2.3	2.6	2.5	2.5
(g/dl)	(0.15)	(0.05)	(0.05)	(0.10)	(0.30)	(0.05)

Values represent mean serum chemistry levels and the standard error of the mean (SEM) values are given in parenthesis.

Compound OCP was found to be non-toxic up to a dose of 160 mg/kg, while HCP–PEG was non-toxic up to a dose of 320 mg/kg, which is in aggrement with the low toxicity observed for other boronated porphyrins of lower boron content [11c, 13–16]. Indeed, these compounds are comparatively less toxic than other previously reported boronated porphyrins, including BTPP, BOPP, ZnDPE and NiNTCP-H [13, 15]. Therefore, porphyrins of high boron content such as OCP and HCP–PEG might be able to deliver high and therapeutic boron concentrations to targeted tumors, which warrants their further evaluation as boron delivery agents for BNCT. Furthermore, conjugation of peptides and other tumor cell-targeting molecules to HCP–PEG might increase its tumor cell uptake and specificity.

EXPERIMENTAL

General

Commercially available reagents and solvents (HPLC grade) were purchased from Sigma-Aldrich and used without further purification. COSAN was purchased from Katchem, Inc. Silica gel 60 (70–230 mesh, Merk) used for column chromatography and silica gel TLC plates (0.2 mm thickness) were purchased from Sorbent Technologies. ^{1}H NMR and ^{13}C NMR spectra were obtained using a Bruker AV-400 MHZ spectrometer; chemical shifts are expressed in ppm. Electronic absorption spectra were measured on a Perkin Elmer Lambda 35 UV-vis spectrophotometer. Mass analysis was conducted at the LSU Mass Spectrometry Facility on a Bruker Omniflex MALDI-TOF mass spectrometer and exact mass were obtained from HRMS-ESI under negative mode on an Applied Biosystems QSTAR XL. Melting points were measured on a Thomas hoover melting point apparatus. Analytical reverse phase HPLC was performed on a Waters system including a 2545 quaternary gradient module pump with a 2489 UV-vis detector and a fraction collector III. Analytical column (4.6X250 mm-XBridge™ BED300 C18 5 μm) and acetonitrile/water solvent system, varying gradient from 100% water (2 min) to 75% acetonitrile/water (5 min) to 100% acetonitrile (10 min). [3,3′-Co(8-$C_4H_8O_2$-1,2-$C_2B_9H_{10}$)(1′,2′-$C_2B_9H_{11}$)] was prepared as previously described [9]. Tetra(3,5-dihydroxyphenyl)porphyrin was purchased from Frontier Scientific and used without further purification in the preparation of OCP, as previously described [5c].

Synthesis

5,10,15-tri(3,5-dimethoxyphenyl)-20-(4-methylesterphenyl)porphyrin (porphyrin 3a). 3,5-dimethoxybenzaldehyde (0.498 g, 3.0 mmol), methyl-4-formyl benzoate (0.246 g, 1.5 mmol), and freshly distilled pyrrole (0.278 mL, 4.0 mmol) were mixed in a 1 L flask. Dry CH_2Cl_2 (500 mL) was added and the mixture stirred under argon for 20 min. $BF_3{\cdot}OEt_2$ (0.16 mL of a 2.5 M solution in CH_2Cl_2) was added at once. The reaction mixture was stirred for 2 h under argon in the dark. DDQ (0.492 g, 2.16 mmol) was added and the stirring continued for 45 min. Then the resulting mixture was neutralized using aqueous $NaHCO_3$ and filtered through a silica gel pad using CH_2Cl_2 as the solvent. The resulting residue was further purified by silica gel column chromatography using CH_2Cl_2/hexanes (9.8:0.2) for elution. The second and main fraction was collected and dried under vacuum (0.09 g, 11%), mp > 300 °C. ^{1}H NMR ($CDCl_3$, 400 MHz): δ, ppm 8.96 (d, J = 7.08 Hz, 6H, β-H), 8.78 (d, J = 4.64 Hz, 2H, β-H), 8.45 (d, J = 8.04 Hz, 2H, o-PhH), 8.31 (d, J = 8.00 Hz, 2H, m-PhH), 7.40 (s, 6H, o-PhH), 6.91 (s, 3H, p-PhH), 4.12 (s, 3H, $COOCH_3$), 3.97 (s, 18H, OCH_3), -2.81 (s, 2H, NH). ^{13}C NMR ($CDCl_3$, 100 MHz): δ, ppm 167.4, 158.9, 147.0, 143.9, 134.5, 131.3, 129.6, 127.9, 120.1, 120.0, 118.6, 113.9, 100.2, 55.6, 52.5. MS (MALDI-TOF): *m/z* 852.779, calcd. for $C_{52}H_{44}N_4O_8$ 852.316. UV-vis (acetone): λ_{max}, nm (ε) 422 (466600), 519 (14500), 553 (1330), 596 (880).

5,10,15-tri(3,5-dimethoxyphenyl)-20-(4-benzyloxyphenyl)porphyrin (porphyrin 3b). 3,5-dimethoxybenzaldehyde (0.498 g, 3.0 mmol), 4-benzyloxybenzaldehyde (0.318 g, 1.5 mmol), and freshly distilled pyrrole (0.278 mL, 4 mmol) were mixed in a 1 L flask. Dry CH_2Cl_2 (500 mL) was added and the solution stirred under argon for 20 min. $BF_3{\cdot}OEt_2$ (0.16 mL of 2.5 M in CH_2Cl_2) was added at once. The reaction mixture was stirred for 2 h under argon and in the dark. DDQ (0.492 g, 2.16 mmol) was added and the stirring continued for 45 min. Then the resulting mixture was neutralized using aqueous $NaHCO_3$ and filtered through a silica gel pad using CH_2Cl_2 as the solvent. The resulting residue was further purified by silica gel column chromatography using CH_2Cl_2/hexanes (9.8:0.2). The main product was isolated and dried (0.09 g, 10%), mp > 300 °C. ^{1}H NMR ($CDCl_3$, 400 MHz): δ, ppm 8.96 (d, J = 7.08 Hz, 6H, β-H), 8.78 (d, J = 4.64 Hz, 2H, β-H), 8.45 (d, J = 8.04 Hz, 2H, o-PhH), 8.31 (d, J = 8.00 Hz, 2H, m-PhH), 7.40 (s, 6H, o-PhH), 6.91 (s, 3H, p-PhH), 4.12 (s, 3H, $COOCH_3$), 3.97 (s, 18H, OCH_3), -2.81 (s, 2H, NH). ^{13}C NMR ($CDCl_3$, 100 MHz): δ, ppm 158.9, 147.2, 142.9, 135.1, 131.2, 129.5, 127.8, 127.2, 120.3, 120.2, 118.6, 113.8, 100.9, 72.0, 55.8. MS (MALDI-TOF): *m/z* 901.358, calcd. for $C_{52}H_{44}N_4O_8$ 901.355. UV-vis (acetone): λ_{max}, nm (ε) 418 (414400), 513 (16100), 553 (4400), 596 (2600).

5,10,15-tri(3,5-dimethoxyphenyl)-20-(4-acetoxyphenyl)porphyrin (porphyrin 3c). 3,5-dimethoxybenzaldehyde (0.498 g, 3.0 mmol), 4-acetoxybenzaldehyde (0.246 g, 1.5 mmol), and freshly distilled pyrrole (0.278 mL, 4.0 mmol) were mixed in a 1 L flask. Dry CH_2Cl_2 (500 mL) was added and the mixture stirred under argon for 20 min. $BF_3{\cdot}OEt_2$ (0.16 mL of 2.5 M in CH_2Cl_2) was added at once. The reaction mixture was stirred for 2 h under argon and in the dark. DDQ (0.492 g, 2.16 mmol) was added and the stirring continued for 45 min. Then the

resulting mixture was neutralized using aqueous $NaHCO_3$ and filtered through a silica gel pad using CH_2Cl_2 as the solvent. The resulting residue was further purified by silica gel column chromatography using CH_2Cl_2/hexanes (9.8:0.2). The main product was isolated and dried (0.102 g, 12%), mp > 300 °C. ^{1}H NMR ($CDCl_3$, 400 MHz): δ, ppm 8.96 (d, *J* = 7.08 Hz, 6H, β-H), 8.78 (d, *J* = 4.64 Hz, 2H, β-H), 8.45 (d, *J* = 8.04 Hz, 2H, o-PhH), 8.31 (d, *J* = 8.00 Hz, 2H, m-PhH), 7.40 (s, 6H, o-PhH), 6.91 (s, 3H, p-PhH), 4.12 (s, 3H, $COOCH_3$), 3.97 (s, 18H, OCH_3), -2.81 (s, 2H, NH). ^{13}C NMR ($CDCl_3$, 100 MHz): δ, ppm 170.0, 158.7, 147.1, 143.7, 134.8, 131.2, 129.0, 127.9, 120.1, 120.0, 118.6, 113.9, 100.2, 55.5, 20.1. MS (MALDI-TOF): *m/z* 852.322, calcd. for $C_{52}H_{44}N_4O_8$ 852.316. UV-vis (acetone): λ_{max}, nm (ε) 419 (426700), 515 (15200), 549 (4200), 588 (2700).

5,10,15-tri(3,5-dihydroxyphenyl)-20-(4-carboxyphenyl)porphyrin. To porphyrin **3a** (0.095 g, 0.1 mmol) in dry CH_2Cl_2 (20 mL) at -20 °C was added dropwise a solution of BBr_3 (0.52 mL, 5.3 mmol) in CH_2Cl_2 (1.5 mL) with vigorous stirring under argon over a period of 30 min. The reaction mixture was stirred at room temperature for 24 h and then poured into water and extracted with ethyl acetate (3 × 50 mL). The combined organic layers were washed successively with brine and aqueous $NaHCO_3$. The organic layer was dried over Na_2SO_4 and evaporated to dryness to give the title porphyrin in 90% yield, mp > 300 °C. ^{1}H NMR (d-acetone, 400 MHz): δ, ppm 9.05 (s, 6H, β-H), 8.86 (s, 2H, β-H), 8.73 (broad s, 6H, OH), 8.50 (d, *J* = 7.88 Hz, 2H, o-PhH), 8.39 (d, *J* = 7.88 Hz, 2H, m-PhH), 7.25 (s, 6H, o-PhH), 6.84 (s, 3H, p-PhH), -2.79 (s, 2H, NH). ^{13}C NMR (d-acetone, 100 MHz): δ, ppm 166.9, 156.8, 146.8, 143.7, 134.5, 130.1, 128.1, 120.4, 120.3, 118.5, 114.5, 102.3. MS (MALDI-TOF): *m/z* 755.432, calcd. for $C_{45}H_{30}N_4O_8$ 755.209. UV-vis (acetone): λ_{max}, nm (ε) 422 (360600), 519 (16700), 553 (5900), 596 (5400), 654 (2800).

5,10,15-tri(3,5-dihydroxyphenyl)-20-[4-carboxy-Gly(Boc)]phenyl)porphyrin (porphyrin 4). To 5,10,15-tri(3,5-dihydroxyphenyl)-20-(4-carboxyphenyl)porphyrin (0.05 g, 0.066 mmol) was added *N*,*N*-diisopropylethylamine (0.0854 g, 0.66 mmol) and 1.5 mL DMF and the resulting mixture was stirred for 5 min. HOBt (0.009 g, 0.066 mmol) and TBTU (0.021 g, 0.066 mmol) were added and the stirring continued at room temperature for 15 min. Glycine *tert*-butyl ester hydrochloride (0.101 g, 0.1 mmol) was added and the final reaction mixture was stirred at room temperature under nitrogen for 48 h. Ethyl acetate was added and the organic solution was washed with brine. The resulting residue was purified by silica gel column chromatography using ethyl acetate for elution. The title porphyrin was obtained in 80% yield, mp > 300 °C. ^{1}H NMR (d-acetone, 400 MHz): δ, ppm 9.05 (s, 6H, β-H), 8.86 (s, 2H, β-H), 8.37 (broad s, 6H, OH), 7.90 (d, *J* = 8.44 Hz, 2H, o-PhH), 7.69 (d, *J* = 8.32 Hz, 2H, m-PhH), 7.26 (s, 6H, o-PhH), 6.85 (s, 3H, p-PhH), 1.54 (s, 9H, $C(CH_3)_3$), -2.79 (s, 2H, NH). ^{13}C NMR (d-acetone, 100 MHz): δ, ppm 169.0, 167.0, 156.7, 145.2, 143.7, 142.9, 134.4, 133.8, 128.3, 127.1, 125.8, 124.5, 120.4, 120.3, 118.9, 118.7, 114.5, 102.3, 80.8, 42.2, 27.4. MS (MALDI-TOF): *m/z* 867.913, calcd. for $C_{51}H_{41}N_5O_9$ 867.290. UV-vis (acetone): λ_{max}, nm (ε) 423 (364000), 519 (18300), 555 (7400), 598 (6000), 654 (3500).

HCP–PEG (porphyrin 2). Porphyrin **4** (14.7 mg, 0.017 mmol) and K_2CO_3 (28.0 mg, 0.20 mmol) were refluxed in 10 mL acetone in a 50 mL round bottom flask under argon for 15 min. The reaction mixture was cooled to room temperature and [3,3′-Co(8-$C_4H_8O_2$-1,2-$C_2B_9H_{10}$)(1′,2′-$C_2B_9H_{11}$)] (42.0 mg, 0.10 mmol) was added. The resulting mixture was stirred at room temperature for 2 h under argon, then refluxed overnight. The second portion of [3,3′-Co(8-$C_4H_8O_2$-1,2-$C_2B_9H_{10}$)(1′,2′-$C_2B_9H_{11}$)] (21.0 mg, 0.05 mmol) was added and reflux continued for 24 h. The last portion of [3,3′-Co(8-$C_4H_8O_2$-1,2-$C_2B_9H_{10}$)(1′,2′-$C_2B_9H_{11}$)] (21.0 mg, 0.05 mmol) was added and reflux continued for an additional 24 h. The reaction was stopped, acetone was evaporated and the resulting solid was washed with diethyl ether several times to remove excess cobaltabisdicarbollide. The resulting orange-red color solid of the corresponding *tert*-butyl-protected porphyrin was kept under vacuum to remove traces of diethyl ether; this porphyrin was obtained (49 mg) in 85% yield. ^{1}H NMR (d-acetone, 400 MHz): δ, ppm 9.01 (s, 6H, β-H), 8.86 (s, 2H, β-H), 8.37 (s, 4H, o,m-PhH), 7.48 (s, 6H, o-PhH), 7.08 (s, 3H, p-PhH), 4.40 (s, 12H, OCH_2), 4.17 (s, 24H, OCH_2), 3.93 (s, 12H, OCH_2), 3.67 (s, 24H, Carb-H), 1.6–3.0 (br, 104, BH, CH_2), 1.54 (s, 9H, $COOC(CH_3)_3$), -2.79 (s, 2H, NH). ^{13}C NMR (d-acetone, 100 MHz): δ, ppm 170.1, 162.0, 158.3, 158.0, 149.9, 145.1, 143.7, 114.5, 101.1, 100.7, 72.2, 69.4, 68.4, 68.0, 59.7, 54.5, 46.6, 28.8. HRMS-ESI: *m/z* 670.4627 [M - 6K + Na]$^{5-}$, calcd. for $[C_{99}H_{209}B_{108}Co_6NaN_5O_{21}]^{5-}$ 670.0437. UV-vis (acetone): λ_{max}, nm (ε) 424 (367702), 519 (7041). To this porphyrin (49 mg, 15 mmol) dissolved in 5 mL of CH_2Cl_2/acetone 1:1, TFA (5 mL) was added and the final mixture was stirred at room temperature for 4 h. The solvents were removed under vacuum and the resulting residue was washed several times with diethyl ether and dried under vacuum. The carboxylated porphyrin was obtained (45 mg) as a green powder in 95% yield. ^{1}H NMR (d-acetone, 400 MHz): δ, ppm 9.01 (s, 6H, β-H), 8.86 (s, 2H, β-H), 8.37 (s, 4H, o,m-PhH), 7.47 (s, 6H, o-PhH), 7.08 (s, 3H, p-PhH), 4.39 (s, 12H, OCH_2), 4.19 (s, 24H, OCH_2), 3.93 (s, 12H, OCH_2), 3.67 (s, 24H, Carb-H), 1.50–2.51 (br, 104, BH, CH_2), -2.79 (s, 2H, NH). HRMS-ESI *m/z* 818.3561 [M - 6K + 2H]$^{4-}$, calcd. for $[C_{95}H_{203}B_{108}Co_6N_5O_{21}]^{4-}$ 818.2954. UV-vis (acetone): λ_{max}, nm (ε) 424 (584300), 520 (28500), 556 (8000), 599 (7700), 655 (2900). This porphyrin (45 mg, 0.013 mmol) was dissolved in DMF (200 μL) and DIEA (13 mg, 0.1 mmol) and the solution stirred at room temperature for 30 min. HOBt (1.84 mg, 0.014 mmol) and HATU (5.18 mg, 0.014 mmol) were added and the mixture was stirred for 1 h. *Tert*-butyl-12-amino-4,7,10-

trioxadodecanoate (4.7 mg, 0.014 mmol) was added to the reaction solution at once and the final mixture was stirred for 72 h at room temperature, under nitrogen. The solvents were evaporated under vacuum and the resulting residue dissolved in ethyl acetate. The organic solution was washed with saturated aqueous NaCl and water. The solvent was evaporated to give a dry residue, which was purified by silica gel column chromatography using acetonitrile/CH_2Cl_2 7:3 as the eluant. The resulting *tert*-butyl-protected porphyrin-PEG was obtained in 20% yield (9.7 mg). ^{1}H NMR (d-acetone, 400 MHz): δ, ppm 9.03 (s, 6H, β-H), 8.88 (s, 2H, β-H), 8.39 (s, 4H, o,m-PhH), 7.47 (s, 6H, o-PhH), 7.07 (s, 3H, p-PhH), 4.38 (s, 12H, OCH_2), 4.24 (s, 24H, OCH_2), 3.93 (s, 12H, OCH_2), 3.66–3.57 (m, 36H, Carb-H, OCH_2), 1.50–2.51 (br, 108, BH, CH_2), -2.79 (s, 2H, NH). HRMS-ESI: *m/z* 714.5167 [M - 5K]$^{5-}$, calcd. for $[C_{108}H_{226}B_{108}Co_6KN_6O_{25}]^{5-}$ 714.0612. UV-vis (acetone): λ_{max}, nm (ε) 424 (455900), 519 (5740), 555 (2500), 598 (2050), 654 (1400). To a solution of the *tert*-butyl-protected porphyrin-PEG (9.7 mg, 0.0025 mmol) in acetone (1 mL), TFA (1 mL) was added and the reaction mixture was stirred at room temperature for 4 h. The solvents were evaporated under vacuum and the resulting solid was washed several times with diethyl ether. After drying, porphyrin **5** was obtained in 95% (9 mg) yield. ^{1}H NMR (d-acetone, 400 MHz): δ, ppm 9.15 (s, 6H, β-H), 9.01 (s, 2H, β-H), 8.61 (s, 4H, o,m-PhH), 7.91 (s, 3H, p-PhH), 7.31 (s, 6H, o-PhH), 4.51 (s, 12H, OCH_2), 4.30 (s, 24H, OCH_2), 4.02 (s, 12H, OCH_2), 3.69 (s, 24H, Carb-H), 3.60 (s, 12H, OCH_2), 1.55–2.85 (br, 108, BH, CH_2). HRMS-ESI: *m/z* 707.1274 [M - 5K - H + Na]$^{5-}$, calcd. for $[C_{104}H_{217}B_{108}Co_6KNaN_6O_{25}]^{5-}$ 707.0457. UV-vis (acetone): λ_{max}, nm (ε) 424 (493600), 519 (25400), 555 (10250), 598 (8350), 654 (5300). HPLC t_R = 8.76.

X-ray crystallographic data

Crystals of porphyrins **3a**, **3b and 3c** for X-ray crystallographic analysis were grown by slow evaporation of their hexane/dichloromethane solutions. Diffraction data were collected at low temperature on a Bruker Kappa Apex-II CCD diffractometer equipped with CuKα radiation (λ = 1.54178 Å) and an Oxford Cryosystems Cryostream chiller. Refinement was by full-matrix least squares using SHELXL [17], with H atoms in idealized positions, guided by difference maps. For porphyrins **3a** and **3c**, the NH hydrogen atoms are disordered, and were placed into four half-populated sites. In porphyrin **3a**, dichloromethane and hexane solvent molecules shared a disordered site on an inversion center. For porphyrin **3c**, electron density amounting to 0.85 molecules of disordered dichloromethane per porphyrin molecule was removed using the SQUEEZE [18] procedure.

Crystallographic data. For **3a**: $C_{52}H_{44}N_4O_8 \cdot 0.307\ C_6H_{14} \cdot 0.386\ CH_2Cl_2$, triclinic space group P-1, a = 9.7437(5), b = 13.4281(10), c = 18.2079(15) Å, α = 87.136(6), β = 78.429(6), γ = 89.623(5)°, V = 2331.0(3) Å^3, T = 90.0(5) K, Z = 2, ρ_{calcd} = 1.300 g.cm^{-3}, μ(CuKα) = 1.10 mm^{-1}. A total of 23,985 data was collected at to θ = 69.0°. R = 0.047 for 7789 data with $Fo^2 > 2\sigma(Fo^2)$ of 8270 unique data and 628 refined parameters, CCDC 824813. For **3b**: $C_{57}H_{48}N_4O_7$, triclinic space group P1, a = 9.420(2), b = 9.786(2), c = 13.609(3) Å, α = 102.099(14), β = 102.101(15), γ = 97.645(15)°, V = 1178.7(4) Å^3, T = 90.0(5) K, Z = 1, ρ_{calcd} = 1.269 g.cm^{-3}, μ(CuKα) = 0.68 mm^{-1}. A total of 14,545 data was collected at to θ = 68.4°. R = 0.065 for 4739 data with $Fo^2 > 2\sigma(Fo^2)$ of 6619 unique data and 619 refined parameters, CCDC 824814. For **3c**: $C_{52}H_{44}N_4O_8 \cdot 0.85\ CH_2Cl_2$, triclinic space group P-1, a = 9.7004(5), b = 13.3343(9), c = 18.2186(10) Å, α = 86.830(5), β = 78.328(5), γ = 89.435(5)°, V = 2304.3(2) Å^3, T = 90.0(5) K, Z = 2, ρ_{calcd} = 1.333 g.cm^{-3}, μ(CuKα) = 1.61 mm^{-1}. A total of 22,993 data was collected at to θ = 68.9°. R = 0.039 for 7440 data with $Fo^2 > 2\sigma(Fo^2)$ of 8188 unique data and 585 refined parameters, CCDC 824815.

Cell studies

All tissue culture media and reagents were obtained from Invitrogen. Human HEp2 cells were obtained from ATCC and maintained in a 50:50 mixture of DMEM:Advanced MEM containing 5% FBS. The cells were sub-cultured biweekly to maintain sub-confluent stocks.

Cytotoxicity. The HEp2 cells were plated at 10 000 per well in a Costar 96 well plate and allowed to grow 36 h. Conjugate stocks 1–5 were prepared in DMSO at a concentration of 10 mM and then diluted into medium to final working concentrations. The cells were exposed to increasing concentrations of HCP–PEG up to 400 μM and incubated overnight. The loading medium was then removed and the cells fed with medium containing Cell Titer Blue (Promega) as per manufacturer's instructions. Cell viability was then measured by reading the fluorescence at 520/584 nm using a BMG FLUOstar plate reader. The signal was normalized to 100% viable (untreated) cells and 0% viable (treated with 0.2% saponin from Sigma) cells. For the phototoxicity experiment the cells were prepared as described above and exposed to HCP–PEG concentrations up to 100 μM. The cells were exposed to a 100 W halogen lamp for 20 min, filtered through a 610 nm long pass filter to provide approximately 1 J/cm^2 light dose. The cells were kept cool by filtering the IR radiation through 10 mm of water and placing the culture in an ice-water bath. After exposure to light, the plate was incubated overnight and the cell viability was measured as described above.

Microscopy. The HEp2 cells were incubated in a glass bottom 6-well plate (MatTek) and allowed to grow for 48 h, before being exposed to 10 μM of HCP–PEG for 6 h. For the co-localization experiments the cells were incubated for 24 h concurrently with porphyrin and one of the following organelle tracers (Invitrogen), for

30 min: ER Tracker Blue/White 100 nM (endoplasmic reticulum), MitoTracker Green at 250 nM (mitochondria), LysoSensor Green at 50 nM (lysosomes), BODIPY FL C_5-ceramide at 50 nM (Golgi network). The slides were washed three times with growth medium and new medium containing 50 mM HEPES pH 7.4 was added. The images were acquired using a Leica DMRXA microscope with 40× NA 0.8 dip objective lens and DAPI, GFP and Texas Red filter cubes (Chroma Technologies).

Animal toxicity

The mice which we used in this project were obtained from the breeding colony operated by the Division of Laboratory Animal Medicine, School of Veterinary Medicine, Louisiana State University. The experiments were conducted according to the guidelines in the protocol approved by Louisiana State University Institutional Animal Care and Use Committee, fully accredited by the Association of Laboratory Animal Care, International. Twelve groups of two BALB/c mice, 4–11 weeks of age and weighing 12–24 g, were used; among these 23 were females and 1 male. Mice in groups 2,3,4,5, and 6 were administrated OCP in 3% DMSO diluted in PBS once *via* ip injection, at increasing dosages; group 2 (20 mg/kg of a 2 mg/mL solution), group 3 (40 mg/kg of a 2 mg/mL solution), group 4 (80 mg/kg of a 4 mg/mL solution), group 5 (120 mg/kg of a 4 mg/mL solution), group 6 (160 mg/kg of a 4 mg/mL solution). Mice in groups 8,9,10,11, and 12 were administrated HCP–PEG in 3% DMSO diluted in PBS, once *via* ip injection, at increasing dosages; group 8 (20 mg/kg of a 2 mg/mL solution); group 9 (40 mg/kg of a 2 mg/mL solution); group 10 (80 mg/kg of a 2 mg/mL solution); group 11 (160 mg/kg of a 20 mg/mL solution); and group 12 (320 mg/kg of a 20 mg/mL solution). Mice in groups 1 and 7 served as vehicle controls and were administered 1.0 mL/25 gms body weight of 3% DMSO, which corresponded to the volume of DMSO injected into mice in group 3. This represented the maximum volume of 3% DMSO injected into any group of mice. Groups of mice were dosed sequentially and each group evaluated daily for signs of toxicity, including hunched posture, rough hair coat, and decreased responsiveness. Mice were anesthetized with CO_2 48 h after compound administration, and blood collected by cardiocentesis for plasma clinical chemistry evaluation. Plasma chemistries performed included glucose, aspartic acid aminotransaminase (AST), alanine aminotransaminase (ALT), alkaline phosphatase (AP), bilirubin, total protein (TP), albumin, and globulin. Mice were exsanguinated and a necropsy performed. Tissues, including lung, kidney, thymus, heart, Harderian gland, spleen, stomach, small intestine and colon were fixed in 10% neutral buffered formalin. Fixed tissues were processed routinely and examined by a board-certified pathologist. For the statistical analysis the clinical chemistry values were compared using the Number Cruncher Statistical System software (NCSS, Kaysville, UT). Variables of interest were statistically evaluated for group effect, using One-Way ANOVA. When the overall F statistic was significant ($p < 0.05$), the Fisher's Least Significant Differences test was performed to compare the groups. Significant differences existed when $p > 0.05$.

CONCLUSION

Two porphyrins of high boron content (34 and 39% boron by weight) were synthesized in high yields, *via* reaction of the corresponding hydrophyphenyl porphyrins with cobaltabisdicarbollide [3,3′-Co(8-$C_4H_8O_2$-1,2-$C_2B_9H_{10}$)(1′,2′-$C_2B_9H_{11}$)]. One of the porphyrins was conjugated to a low molecular weight PEG group to increase its solubility and to provide a spacer for future conjugations to peptides and other molecules. OCP showed no cytotoxicity towards human HEp2 cells at concentration up to 50 μM; at higher concentrations compound precipitation was observed. On the other hand HCP–PEG was found to be non-toxic up to 400 μM in the dark, and up to 100 μM after exposure to 1 J/cm^2 light dose. The preferential sites of subcellular localization were found to be the lysosomes, maybe as a result from an endocytic internatization mechanism. No signs of toxicity were observed in BALB/c mice upon single ip injection of high doses of these porphyrins. The determined MTD values for OCD and HCP–PEG were 160 mg/kg and 320 mg/kg, respectively. Such low toxicity warrants further evaluation of these porphyrins of high boron content as boron delivery vehycles for BNCT, and these studies are currently underway in our laboratories.

Acknowledgements

The work described was supported by the US National Institutes of Health, grant number R01 CA098902.

Supporting information

Crystallographic data have been deposited at the Cambridge Crystallographic Data Centre (CCDC) under numbers CCDC 824813–824815. Copies can be obtained on request, free of charge, *via* www.ccdc.cam.ac.uk/conts/retrieving.html or from the Cambridge Crystallographic Data Centre, 12 Union Road, Cambridge CB2 1EZ, UK (fax: +44 1223-336-033 or email: deposit@ccdc.cam.ac.uk).

REFERENCES

1. a) Hawthorne MF. *Angew. Chem. Int. Ed. Eng.* 1993; **32**: 950. b) Soloway AH, Tjarks W, Barnum BA, Rong FG, Barth RF, Codogni IM and Wilson JG. *Chem. Rev.* 1998; **98**: 1515. c) Barth RF, Soloway AH, Goodman JH, Gahbauer RA, Gupta N, Blue TE, Yang WL and Tjarks W. *Neurosurg.* 1999; **44**: 433.

2. a) Barth RF, Coderre JA, Vicente MGH and Blue TE. *Clinical Cancer Research* 2005; **11**: 3987. b) Sibrian-Vazquez M and Vicente MGH. In *Boron Science: New Technologies & Applications*, Hosmane NS. (Ed.) CRC Press: 2011; pp 203.
3. Barth RF and Joensuu H. *Rad. Oncol.* 2007; **82**: 119.
4. Vicente MGH and Sibrian-Vazquez M. In *The Handbook of Porphyrin Science*, Vol 4, Kadish KM, Smith KM and Guilard R. (Eds.) World Scientific Publishers: Singapore, 2010; pp 191.
5. a) Hao E and Vicente MGH. *Chem. Commun.* 2005: 1306. b) Hao E, Jensen TJ, Courtney BH and Vicente MGH. *Bioconjugate Chem.* 2005; **16**: 1495. c) Hao E, Sibrian-Vazquez M, Serem W, Garno JC, Fronczek FR and Vicente MGH. *Chem. Eur. J.* 2007; **13**: 9035. d) Sibrian-Vazquez M, Hao E, Jensen TJ and Vicente MGH. *Bioconjugate Chem*. 2006; **17**: 928. e) Hao E, Zhang M, E WB, Kadish KM, Fronczek FR, Courtney BH and Vicente MGH. *Bioconjugate Chem.* 2008; **19**: 2171.
6. a) Lindsey JS, Hsu HC and Schreiman IC. *Tetrahedron Lett.* 1986; **27**: 4969. b) Lindsey JS and Schreiman IC. *J. Org. Chem*. 1987; **52**: 827.
7. Sibrian-Vazquez M, Jensen TJ and Vicente MGH. *J. Med. Chem*. 2008; **51**: 2915.
8. Sibrian-Vazquez M, Jensen TJ, Fronczek FR, Hammer RP and Vicente MGH. *Bioconjugate Chem.* 2005; **16**: 852.
9. Teixidor F, Pedrajas J, Rojo I, Vinas C, Kivekas R, Sillanpaa R, Sivaev I, Bregadze V and Sjoberg S. *Organometallics* 2003; **22**: 3414.
10. Zhang JH, Chung TD and Oldenburg KR. *J. Biomol. Screen.* 1999; **4**: 67.
11. a) Vicente MGH, Edwards BF, Shetty SJ, Hou Y and Boggan JE. *Bioorg. Med. Chem*. 2002; **10**: 481. b) Gottumukkala V, Luguya R, Fronczek FR and Vicente MGH. *Bioorg. Med. Chem*. 2005; **13**: 1633. c) Gottumukkala V, Ongayi O, Baker DG, Lomax LG and Vicente MGH. *Bioorg. Med. Chem*. 2006; **14**: 1871.
12. a) Woodburn K, Phadke AS and Morgan AR. *Bioorg. Med. Chem. Lett.* 1993; **3**: 2017. b) Nguyen T, Brownell GL, Holden SA and Teicher BA. *Biochem. Pharm.* 1993; **45**: 147. c) Callahan DE, Forte TM, Afzal SMJ, Deen DF, Kahl SB, Bjornstad KA, Bauer WF and Blakely EA. *Int. J. Rad. Oncol. Biol. Phys.* 1999; **45**: 761.
13. a) Miura M, Micca PL, Fisher CD, Heinrichs JC, Donaldson JA, Finkel GC and Slatkin DN. *Int. J. Cancer*. 1996; **68**: 114. b) Miura M, Micca PL, Fisher CD, Gordon CR, Heinrichs JC and Slatkin DN. *Br. J. Radiol*. 1998; **71**: 773. c) Miura M, Micca PL, Heinrichs JC, Gabel D, Fairchild RG and Slatkin DN. *Biochem. Pharmacol*. 1992; **43**: 467.
14. a) Vicente MGH, Wickramasighe A, Nurco DJ, Wang HJH, Nawrocky MM, Makar MS and Miura M. *Bioorg. Med. Chem*. 2003; **11**: 3101.
15. a) Kahl SB, Joel DD, Nawrocky MM, Micca PL, Tran KP, Finkel GC and Slatkin DN. *Proc. Natl. Acad. Sci. U.S.A*. 1990; **87**: 7265. b) Zhou R, Balasubramanian SV, Kahl SB and Straubinger RM. *J. Pharm. Sci*. 1999; **88**: 912. c) Tibbitts J, Fike JR, Lamborn KR, Bollen AW and Kahl SB. *Photochem. Photobiol*. 1999; **69**: 587.
16. Hao E, Friso E, Miotto G, Jori G, Soncin M, Fabris C, Sibrian-Vazquez M and Vicente MGH. *Org. Biomol. Chem*. 2008; **20**: 3732.
17. Sheldrick GM. *Acta Crystallogr. Sect. A* 2008; **64**: 112.
18. Spek AL. *Acta Crystallogr. Sect. D-Biol. Crystallogr.* 2009; **65**: 148.

